Evolution of β-lactam resistance causes fitness reductions and several cases of collateral sensitivities in the human pathogen *Haemophilus influenzae*

Sabine Petersen[1], Margo Diricks[2,3], Christian Utpatel [2], Hinrich Schulenburg[4,5], Matthias Merker[1,3]

[1] Evolution of the Resistome, Research Center Borstel, Borstel, Germany

[2] Molecular and experimental Mycobacteriology, Research Center Borstel, Borstel, Germany

[3] German Center for Infection Research, Partner site Hamburg-Lübeck-Borstel-Riems, Borstel-Lübeck, Germany

[4] Evolutionary Ecology and Genetics, Kiel University, Kiel, Germany

[5] Antibiotic Resistance Group, Max-Planck Institute for Evolutionary Biology, Ploen, Germany

Correspondence to: Prof. Matthias Merker, Research Center Borstel, Leibniz Lung Center, Parkallee 1, 23845 Borstel, phone: +49-4537188-7570, e-mail: mmerker@fz-borstel.de

Short title: β-lactam Resistance Drives Trade-offs in H. influenzae

Transparency declarations: The authors declare that they do not have any competing interests.

Keywords: Haemophilus influenzae, ampicillin resistance, cephalosporine resistance, evolution of antimicrobial resistance, collateral effects

Abstract

The evolution of antimicrobial resistant (AMR) pathogens poses a global health threat and it is unclear if evolutionary trajectories to resistance lead to predictable phenotypes. We analyzed AMR-evolution in the human pathogen *Haemophilus influenzae* in controlled evolution experiments with increasing concentrations of either ampicillin, cefotaxime, or ceftriaxone. We isolated 315 clones from different time points of six independent experiments and characterized changes in genome sequences, bacterial fitness, and minimum inhibitory concentrations (MICs) to 14 antibiotics. Resistance evolution under ampicillin and cefotaxime was driven by mutations in the *ftsI* gene, encoding the penicillin-binding protein 3. However, ceftriaxone exposure mainly selected for mutations in the outer membrane protein P2 (OmpP2). Some OmpP2-mutants reproducibly showed heteroresistance for ceftriaxone but also for fluoroquinolones, rifampicin and tetracycline. Bacterial fitness assessments revealed trade-offs between resistance-associated mutations and growth, though no systematic correlation of MIC increase and growth deficit was detected. Over 50% of the mutants became more susceptible to aminoglycosides, clarithromycin, and colistin, while some mutation patterns resulted in cross-resistance to meropenem and fluoroquinolones. Overall, beta-lactam antibiotics reproducibly selected mutants with increased MICs, but evolutionary pathways and resulting phenotypes remain unpredictable, challenging current AMR treatment guidelines, and recommendations for last resort antibiotics.

56 ## Introduction

57 Antimicrobial resistance (AMR) is a major public health challenge globally (1). The WHO has identified
58 several priority pathogens to inform research and development as well as public health interventions
59 to combat the AMR crisis (2). One of these priority pathogens are ampicillin resistant *Haemophilus*
60 *influenzae* strains. *H. influenzae* is a common Gram-negative opportunistic pathogen residing in the
61 human upper respiratory tract (3,4). The bacterium can cause a range of infections, from mild illnesses
62 like sinusitis and otitis media to severe invasive diseases such as meningitis and bacteremia,
63 particularly in vulnerable populations (5). Despite the successful implementation of a vaccine against
64 *H. influenzae* serotype b strains, non-typeable strains (NTHi), i.e. strains lacking a polysaccharide
65 capsule, have become prevalent (6) and evolved resistance to aminopenicillins such as ampicillin and
66 amoxicillin in many world regions (7–9).

67 Thus, third generation cephalosporins such as cefotaxime, and ceftriaxone, are becoming more and
68 more important for treating ampicillin resistant *H. influenzae* infections (10) as they overcome
69 ampicillin resistance mediated by the beta-lactamases TEM-1 and ROB-1 (11,12). However, resistance
70 to ampicillin can also evolve in beta-lactamase negative strains via alterations in the penicillin binding
71 protein 3 (PBP3), encoded by the *ftsI* gene (13). Mutations in *ftsI*, particularly in the transpeptidase
72 domain of PBP3, reduce the binding affinity for different beta-lactam antibiotics (14).

73 Current understanding is limited regarding whether resistance evolution in *H. influenzae* follows
74 identical genetic and phenotypic trajectories across different beta-lactam classes, and whether such
75 evolutionary pathways are reproducible. In particular, it is unclear if evolution consistently leads to
76 cross-resistances against multiple beta-lactam antibiotics, or if variability in resistance mechanisms
77 leads to diverse outcomes. Here, laboratory-based evolution experiments provide a powerful
78 approach to address these questions (15). By simulating selective pressures *in vitro*, these experiments
79 allow for tracking genetic changes and phenotypic adaptations as resistance evolves. In addition, this
80 experimental approach facilitates an assessment of evolved collateral effects, such as cross-resistance
81 or collateral sensitivity (i.e., variants with evolved resistance against certain antibiotics show an
82 increase in susceptibility to other antibiotics), which may inform about epistatic interactions, and
83 possibly new treatment regimens against resistant strains (16).

84 Therefore, the aim of the current study was to enhance our understanding on the predictability of
85 resistance evolution and the resulting collateral effects. In particular, we investigated the evolutionary
86 pathways leading to resistance against either ampicillin, cefotaxime, or ceftriaxone in *H. influenzae*
87 using a multi-step *in vitro* evolution approach. By subjecting the reference strain *H. influenzae* Rd KW20
88 to increasing concentrations of these antibiotics, we tested whether evolution results in identical or
89 divergent genetic trajectories and phenotypes. We employ short and long read sequencing
90 technologies to map mutations across the genome and assess their impact on minimum inhibitory

91 concentrations (MICs) for different antibiotics. Furthermore, we evaluated whether the evolution of
92 resistance is reproducible by examining the consistency of mutation patterns and collateral effects on
93 other antibiotics.

94 Methods

95 Bacteria and culture methods

96 The beta-lactamase negative reference strain *H. influenzae* Rd KW20 and evolved mutant strains were
97 routinely grown from -80°C freezer stocks on chocolate agar (Mueller-Hinton broth with 5 g/L yeast
98 extract, 17 g/L agar, 5% defibrinated horse blood and 20 mg/L beta-nicotinamide adenine dinucleotide
99 (beta-NAD)) at 37°C in a humid atmosphere containing 5% CO_2. Colonies grown on chocolate agar
100 served as inoculum for liquid cultures in Mueller-Hinton broth supplemented with 5 g/L yeast extract,
101 20 mg/L beta-NAD and 15 mg/L hemin, hereafter referred to as *Haemophilus* test medium (HTM),
102 grown at 37°C and shaking at 100 or 200 rpm. Liquid cultures were routinely plated on HTM agar
103 (formulation of HTM with 17 g/L agar added).

104 Antibiotic susceptibility testing

105 To determine the antibiotic starting concentrations for the multi-step evolution experiment, MICs of
106 ampicillin, cefotaxime and ceftriaxone were tested for the reference strain using broth microdilution
107 methodology according to EUCAST protocol, but using HTM. Ampicillin sodium salt, cefotaxime sodium
108 salt, and ceftriaxone disodium salt hemi(heptahydrate) were purchased from Sigma-Aldrich.

109 Gradient diffusion strips (Liofilchem® MIC Test Strips) on Mueller Hinton fastidious agar (MH-F, BD)
110 were routinely used for all isolated single clones evolved in the evolution experiment to determine
111 MICs of ampicillin, cefotaxime and ceftriaxone. To check for collateral effects, 17 clones were
112 additionally tested for clarithromycin, kanamycin, colistin, vancomycin, levofloxacin, rifampicin,
113 amikacin, tetracycline, gentamicin and meropenem susceptibility using Liofilchem® MIC Test Strips.
114 Susceptibility interpretation was performed according to EUCAST breakpoints v. 13.0 2023, which are
115 1 mg/L for ampicillin, 0.125 mg/L for cefotaxime, and 0.125 mg/L for ceftriaxone.

116 Multi-step evolution experiment

117 Populations of the susceptible reference strain *H. influenzae* Rd KW20 were evolved under antibiotic
118 pressure (ampicillin, cefotaxime, ceftriaxone) in HTM, starting with an antibiotic concentration of
119 0.5xMIC of the reference strain (determined using broth microdilution methodology). One population
120 was evolved in the absence of any antibiotic pressure (control). Evolution in the presence of
121 ceftriaxone was performed three times to investigate reproducibility of resistance evolution.

122 A volume of 20 µL of single colony resuspension (one single colony of *H. influenzae* Rd KW20 grown on
123 chocolate agar resuspended in 100 µL of HTM) was used to inoculate 2-mL cultures containing either

124 0.125 mg/L of ampicillin, 0.008 mg/L of cefotaxime, 0.002 mg/L of ceftriaxone (0.002 mg/L) or no
125 antibiotic (1st passage) (Supplementary Figure S1).

126 The evolving 2-mL cultures were grown in 12-well microtiter plates at 37°C, 100 rpm and 5% CO_2 for
127 four days per cycle, with daily 100-fold dilution into 2 mL of fresh HTM. At each passage, one culture
128 was grown at the same antibiotic concentration as in the previous passage (back-up culture), while
129 three additional cultures were inoculated containing twice the antibiotic concentration of the previous
130 passage. Whenever at least one of the cultures with higher antibiotic concentration showed visible
131 growth after 24 h, this culture was used to inoculate the next passage. This approach allowed for a
132 stepwise increase in antibiotic concentration throughout the experiment without extinction. At the
133 end of each four-day cycle, 20 µL of culture were spotted onto chocolate agar and incubated for three
134 days at 37°C and 5% CO_2. After incubation, the biomass of the spotted cultures was resuspended in 1
135 mL of HTM, and 20 µL of this resuspension were used to initiate the next cycle. This process was
136 repeated for a total of five cycles adding up to twenty passages in liquid medium. In the final cycle,
137 cultures were not spotted onto chocolate agar but directly processed. Glycerol stocks (HTM with 20%
138 glycerol) of each passage were stored at -80°C.

139 Single clones were isolated from each passage by dilution streaking of the respective glycerol stocks
140 on chocolate agar. In general, two clones were isolated per passage. However, whenever the antibiotic
141 concentration was increased compared to the previous passage, five clones were isolated instead.
142 Isolated clones were grown in 3 mL of HTM to determine MICs of ampicillin, cefotaxime, and
143 ceftriaxone using gradient diffusion strips (Liofilchem® MIC Test Strips) and to isolate DNA using the
144 DNeasy UltraClean Microbial Kit (Qiagen) for DNA sequencing.

145 Whole genome sequencing

146 Short read DNA-libraries were prepared from extracted genomic DNA with a modified Illumina Nextera
147 XT library kit protocol as described previously (17). Libraries were sequenced with 150 bp paired-end
148 reads on an Illumina NextSeq 2000 (Illumina, San Diego, CA, USA). Short read data (fastq files) are
149 available in the European Nucleotide Archieve (ENA) under the BioProject PRJEB86018. Accession
150 numbers are available in Supplementary Table S1. Mutations, i.e. single nucleotide polymorphisms
151 (SNPs), short insertions and deletions, were called with a reference mapping pipeline (18). Briefly,
152 short reads were mapped to the reference genome *H. influenzae* Rd KW20 (ATCC 51907) (BioSample
153 SAMN39831887) using the Burrows-Wheeler Aligner (BWA) (19) and allele calling was done with the
154 Genome Analysis Toolkit (GATK) (20). Mutations were called with the following thresholds: 4 reads
155 mapped in both forward and reverse orientation, a minimum of 8 reads with a PHRED score ≥20 and
156 ≥75% allele frequency. Indels in the gene *hdsM* (i.e. repetitive region) were excluded. For subsequent
157 phylogenetic analysis, SNPs were concatenated when at least 95% of all isolates fulfilled the

158 abovementioned thresholds for read coverage, PHRED score and frequency at individual genome
159 positions.

160 Long read sequencing was performed with the PacBio Sequel II system (Pacific Biosciences, CA, USA)
161 for selected clones at different timepoints from each evolution experiment to identify structural
162 genomic changes. DNA libraries were prepared with the SMRTbell Express Template Prep Kit 2.0 with
163 barcoded adapters from IDT (Integrated DNA Technologies, USA). Alignment files (.bam) are available
164 in the ENA under the BioProject PRJEB86018. De-novo genome assembly was performed using the
165 PacBio SMRTlink software v9.0 and its "Microbial Assembly" application, with the genome length set
166 to 1.8 Mb and a seed coverage of 30. For the resulting assemblies, the same origin was set using the
167 first 50 bp of dnaA. This sequence was identified using the Seqkit toolkit (Seqkit v2.9.0), and the origin
168 was adjusted accordingly. Subsequently, each assembly was aligned to the reference genome using
169 progressiveMauve (Mauve v2.4.0), and the detected variations were extracted from the alignment.
170 Indels of at least four bases in length were further examined through visual inspection of the assembly
171 and reference mapping in these regions to characterize the mutation more precisely (tandem repeat
172 variation, inversion, deletion, insertion).

173 Long read sequencing detected deletions and inversions in *ompP2*, which were not detected using
174 Illumina sequencing. To check for presence of structural changes affecting *ompP2* the BWA alignment
175 files of all 315 clones were checked manually for variations in *ompP2* using Geneious Prime v2024.0.5
176 (https://www.geneious.com/).

177 ## Phylogenetic and Bayesian analysis

178 Fasttree v.2.1.9 (21) was used to calculate phylogenetic trees for each evolution experiment with a
179 general time reversible (GTR) substitution model and Gamma20 likelihood optimization to account for
180 evolutionary rate heterogeneity among sites and 500 bootstrap replicates. Figtree v.1.4.4
181 (https://github.com/rambaut/figtree/releases) was used to root phylogenetic trees at midpoint and
182 iTol v.6.8.1 (https://itol.embl.de/) was used for visualization. A phylogenetic molecular clock signal was
183 first assessed with TempEst v1.5 (22) by the correlation of sampling day and root-to-tip distance. We
184 further performed a permutation-based linear regression analysis using the lmPerm v2.1.0 R package,
185 to tests the significance of the regression model without assuming normality by computing p-values
186 through randomized permutations of the data. Mutation rates were calculated with BEAST2.5 (23) for
187 all evolution experiments, except one replicate experiment exposed to ceftriaxone with a poor
188 correlation of SNPs and sampling time, and a non-converging Markov-Chain-Monte-Carlo sampling.
189 We employed a coalescent exponential population model, log normal clock rate, a strict molecular
190 clock, tip dating (day of the experiment), a GTR substitution model, 20 million iterations with 10% burn-
191 in, and sampling every 2,000 traces/trees. Inspection of BEAST log files with Tracer v1.7.2 showed an

192 adequate mixing of the Markov chains and all parameters were observed with an effective sample size
193 (ESS) >200.

194 Competitive growth assay

195 Pairwise competitive growth assays were performed to estimate the *in vitro* relative fitness of mutants
196 evolved in the multi-step evolution experiment compared to the parental strain (*H. influenzae* Rd
197 KW20). Briefly, five single colonies grown on chocolate agar served as inoculum for 3 mL pre-cultures
198 that were grown until mid-exponential phase (Supplementary Figure S2). Pre-cultures were diluted to
199 an OD_{600} of around 0.025. Equal volumes (1.5 mL) of diluted mutant and parental strain cultures were
200 added in 15 mL falcon tubes. Co-cultures were grown in triplicate for 4 h at 37°C and shaking at 200
201 rpm. Initial and final colony forming units (CFU) of the mutant and parental strain were determined by
202 standard plate counting on HTM agar (total CFU) and on HTM agar containing 0.016 g/mL cefotaxime
203 (mutant CFU), respectively. Even though co-cultures were inoculated to a 1:1 ratio of the OD_{600} of the
204 two competing strains, initial CFU counts sometimes differed between both strains. Initial CFU ratios
205 of the parental strain to that of the mutant strain of 1:0.5 to 1:2 were accepted, as the formula used
206 below accounts for unequal starting CFUs. Relative fitness was assessed as the ratio of the Malthusian
207 parameter of the mutant to that of the parental (reference) strain. The following formula considering
208 population sizes of the mutant and the parental strain was used for the calculation of fitness of each
209 strain in relation to the parental strain (24).

$$fitness_m = \frac{\ln\left(\frac{A_{m,\,4h}}{A_{m,\,0h}}\right)}{\ln\left(\frac{A_{r,\,4h}}{A_{r,\,0h}}\right)}$$

210 The formula calculates the fitness ($fitness_m$) of the mutant strain relative to the reference strain (Rd
211 KW20). Here, A represents the population size, with subscripts m for the mutant strain and r for the
212 reference strain. The time points 0h and 4h indicate the population size at inoculation and after 4
213 hours, respectively. A fitness of 1 indicates no fitness cost, whereas a ratio greater than or less than 1
214 indicates increased or decreased fitness compared to the parental strain, respectively. A one-sample
215 t-test (considering the Malthusian parameters $\ln(A_{m,\,4h}/A_{m,\,0h})$ and $\ln(A_{r,\,4h}/A_{r,\,0h})$) with Benjamini
216 Hochberg correction for multiple testing was used to assess the significance of fitness gain/loss of
217 mutants compared to the reference strain. Pairwise t-tests with with Benjamini-Hochberg correction
218 were conducted to identify significant differences between fitness values of clones isolated from the
219 same evolving population.

220 Crystal structures

221 The crystal structure of the transpeptidase domain (amino acid 254-610) of PBP3 of *H. influenzae* was
222 obtained from the RCSB Protein Data Bank (entry ID 6HZO deposited by Bellini et al.). Detected PBP3

223 substitutions were visualized in this crystal structure using PyMOL v3.0 (https://www.pymol.org/).
224 Ampicillin and cefotaxime were superimposed using crystal structures of PBP3 of *Mycobacterium*
225 *tuberculosis* (entry ID 6KGW) and *Staphylococcus aureus* (entry ID 3VSL). Structure of full PBP3 (entry
226 ID AF-P45059-F1-v4) was obtained from AlphaFold Protein Structure Database.

227 AlphaFold Server powered by AlphaFold 3 (25) was used to predict structures of wild-type and mutated
228 Outer membrane protein P2 (OmpP2). Predicted structures were visualized using PyMOL v3.0.

229 Statistical analyses

230 The association between specific mutations and a reduction in susceptibility was analyzed using Mann-
231 Whitney U tests. For this purpose, the ampicillin, cefotaxime, and ceftriaxone MIC values of two sets
232 of evolved clones were compared. The clones in the two sets differed genetically only by the mutation
233 or mutation combination under investigation (based on short read sequencing approach and the
234 manual check of *ompP2* mutations in the BWA alignments), aside from detected tandem repeat
235 variations in the *hsdM* gene. For each clone set, a minimum of three genetically identical clones was
236 required. To minimize the risk of false-positive results due to multiple testing, p-values were adjusted
237 using the Benjamini-Hochberg correction.

238 A permutation test was conducted to evaluate the association between average fitness and
239 antimicrobial susceptibility (MIC) to ampicillin, cefotaxime, and ceftriaxone. For each antibiotic, the
240 observed correlation between relative fitness value and MIC was calculated. The null distribution was
241 generated by randomly shuffling the MIC values within each group and recalculating the correlation
242 for 10,000 permutations. The p-value was determined by comparing the observed correlation to the
243 null distribution, assessing the statistical significance of the observed association.

244 Results

245 Evolution of beta-lactam resistance is mainly driven by *ftsI* and *ompP2* mutations

246 We exposed the reference strain *H. influenzae* Rd KW20 in a multi-step evolution experiment to
247 increasing concentrations of the three beta-lactam antibiotics ampicillin, cefotaxime and ceftriaxone.
248 Bacterial populations evolved over 20 transfers in individual experiments, which is equivalent to
249 approximately 200 generations. Overall, we investigated the genomes and MICs of 315 clones, isolated
250 across time from six independent evolution experiments including a drug free control and three
251 replicate experiments with ceftriaxone. We identified between 11 and 25 mutations (including SNPs,
252 and indels) in individual experiments over 20 days of exponential growth, resulting in a linear increase
253 in the number of mutations across time. SNP based phylogenies and root-to-tip linear regressions (R2
254 0.31-0.86) indicated moderate to strong support of a constant molecular clock in all evolution
255 experiments, except for one replicate exposed to ceftriaxone (R2=0.11) (Supplementary Table S3).

256 Based on a Bayesian coalescent model, assuming a strict molecular clock and exponential population
257 growth, the mutation rates ranged from 1.0 x 10^{-7} to 2.1 x 10^{-7} substitutions per site per day.

258 The MICs against the three beta-lactam antibiotics of individual clones did not change significantly in
259 the drug-free control experiment. In the drug free control, measured MIC differences were within the
260 range of technical variation, i.e. one doubling dilution compared to the MICs of the parental strain Rd
261 KW20 which were 0.19 mg/L for ampicillin, 0.008 mg/L for cefotaxime, and 0.003 mg/L for ceftriaxone.
262 (Supplementary Figure S3). We also did not detect any mutations in the main drug target *ftsI* in the
263 evolved control population (Supplementary Table S1).

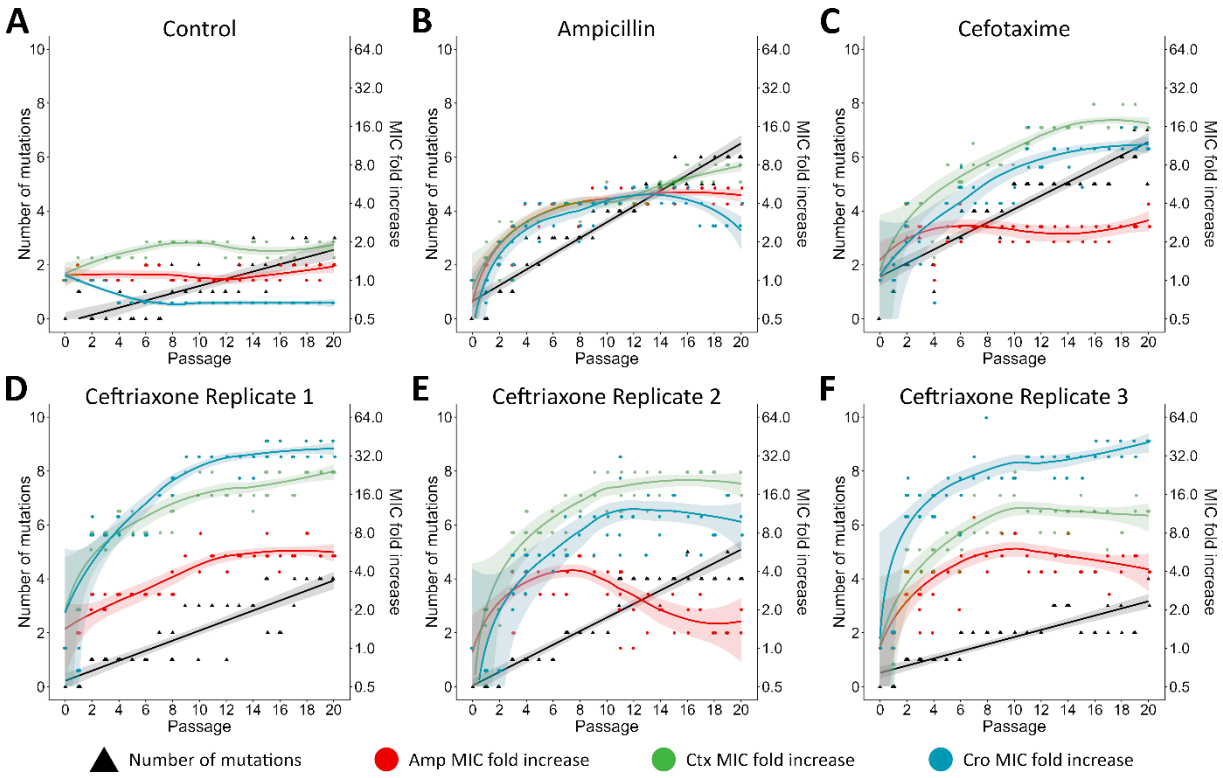

264

265 Figure 1: Increasing number of mutations and changes of beta-lactam MICs in six evolution experiments. Number of
266 mutations (black) and minimum inhibitory concentration fold-increase compared to the parental strain Rd KW20 for
267 ampicillin (Amp, red), cefotaxime (Ctx, green), and ceftriaxone (Cro, blue) in selected clones over 20 passages (two or five
268 clones per passage). Bacterial population A - without antibiotic exposure and exposed to increasing concentrations of B -
269 ampicillin, C - cefotaxime, D - ceftriaxone replicate 1, E - ceftriaxone replicate 2, F - ceftriaxone replicate 3. Shaded areas
270 represent the 95% confidence interval.

271 In contrast, exposure to ampicillin, cefotaxime and ceftriaxone resulted in significantly increased beta-
272 lactam MICs (Figure 1). Specifically, exposure to ceftriaxone led to strong MIC increases, including in
273 one clone an MIC increase of up to 64-fold against ceftriaxone relative to the ancestor strain. Exposure
274 to ampicillin resulted in more moderate MIC increases against all three beta-lactam antibiotics.

275 Furthermore, populations exposed to third-generation cephalosporins showed a more pronounced
276 MIC increase against ceftriaxone and cefotaxime as compared to ampicillin.

277 Clinical resistance against cefotaxime (EUCAST breakpoint: > 0.125 mg/L) was observed for 4/55 (7.3%)
278 clones evolved under cefotaxime exposure and for 28/169 (16.6%) clones evolved in three evolution
279 experiments under ceftriaxone exposure (Figure 2, Supplementary Figure S3). Exposure to ceftriaxone
280 further selected 1/169, (0.6%) ceftriaxone resistant (EUCAST breakpoint: > 0.125 mg/L) clone and
281 10/169 (5.9%) ampicillin resistant (EUCAST breakpoint: > 1 mg/L) clones. Cross-resistance against
282 ampicillin and cefotaxime was observed for five clones evolved under ceftriaxone exposure
283 (Supplementary Figure S3). Overall, 20 days exposure to ampicillin did not select for clinical resistant
284 clones against any of the three tested drugs.

285 As expected, increasing MICs against the beta-lactam antibiotics were associated with mutations in *ftsI*
286 (Figure 2, Supplementary Figure S3). Specifically, we identified combinations of the following five
287 amino acid (amino acid) substitutions in individual clones in the transpeptidase domain: p.Thr332Ile
288 (c.968C>T), p.Thr443Ala (c.1327A>G), p.Ala530Ser (c.1591G>T), p.Asp551Tyr (c.1652G>T), and
289 p.Ala561Glu (c.1684C>A). Exposure to both ampicillin and cefotaxime, selected for p.Ala530Ser. Under
290 cefotaxime conditions p.Ala530Ser, p.Thr443Ala, and p.Thr332Ile evolved in a stepwise manner. The
291 substitutions p.Asp551Tyr and p.Ala561Glu were detected independently in separate clones each
292 arising contemporaneously (detected in 3rd passage) in one population exposed to ceftriaxone. The
293 detected *ftsI* mutations were significantly associated with MIC increase of beta-lactams
294 (Supplementary Table S4). In a crystal structure model of PBP3, all five *ftsI* mutations were either in
295 proximity to other well-known resistance associated amino acid positions (Ile449, Arg517, Asn526), or
296 close to the binding site of the antibiotics (Figure 3).

297

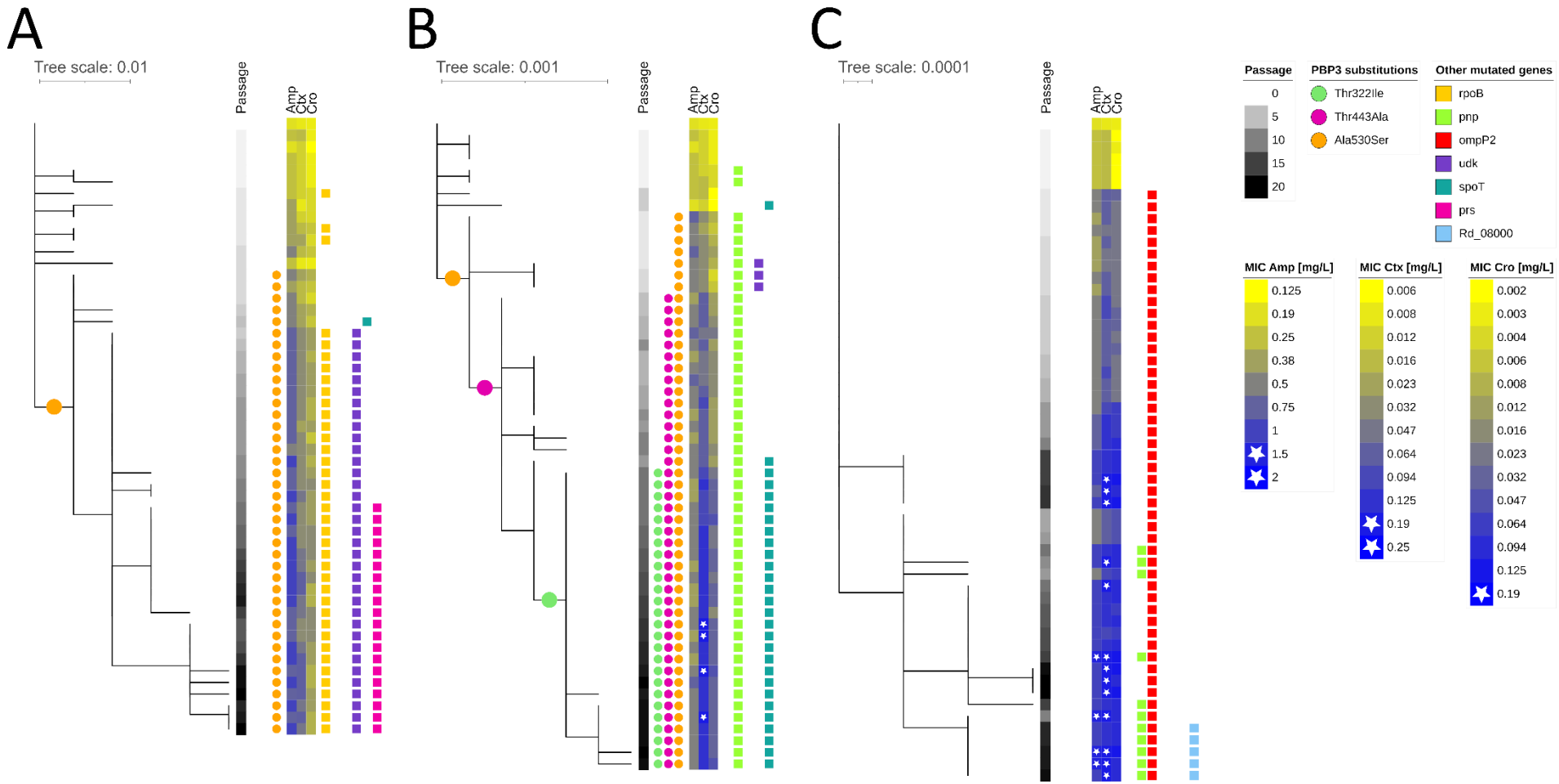

Figure 2: Maximum likelihood phylogeny of *H. influenzae* Rd KW20 clones evolved in the presence of ampicillin (A, 53 clones), cefotaxime (B, 56 clones), and ceftriaxone (C, 57 clones). Amino acid substitutions in the penicillin binding protein 3 (PBP3) and presence of mutations in specified genes as well as minimum inhibitory concentration (MIC) changes over time are color coded. Strains that exceeded the clinical breakpoint for ampicillin/cefotaxime/ceftriaxone according to EUCAST breakpoints are marked with a white star at the MIC heatmap.
The specified genes are those in which at least 20 clones from the whole set of selected clones exhibited mutations but did not mutate under antibiotic-free conditions.

299 Furthermore, *ftsI* mutations differentially affected the susceptibility against ampicillin, cefotaxime, and
300 ceftriaxone. While we observed a significant MIC increase for ampicillin (2-fold increase, p_{adj} = 0.008)
301 and ceftriaxone (3-fold increase, p_{adj} = 0.004) associated with amino acid substitution p.Ala530Ser, the
302 secondary amino acid substitution p.Thr443Ala did not significantly affect ampicillin susceptibility but
303 was associated with a two-fold increase of the MIC towards cefotaxime (p_{adj} = 0.019) (Supplementary
304 Table S4). Out of the five detected PBP3 substitutions, p.Asp551Tyr showed the highest MIC fold
305 increase towards all three beta-lactams with a maximum 8-fold increase of the MIC of ceftriaxone (p_{adj}
306 = 2E-06).

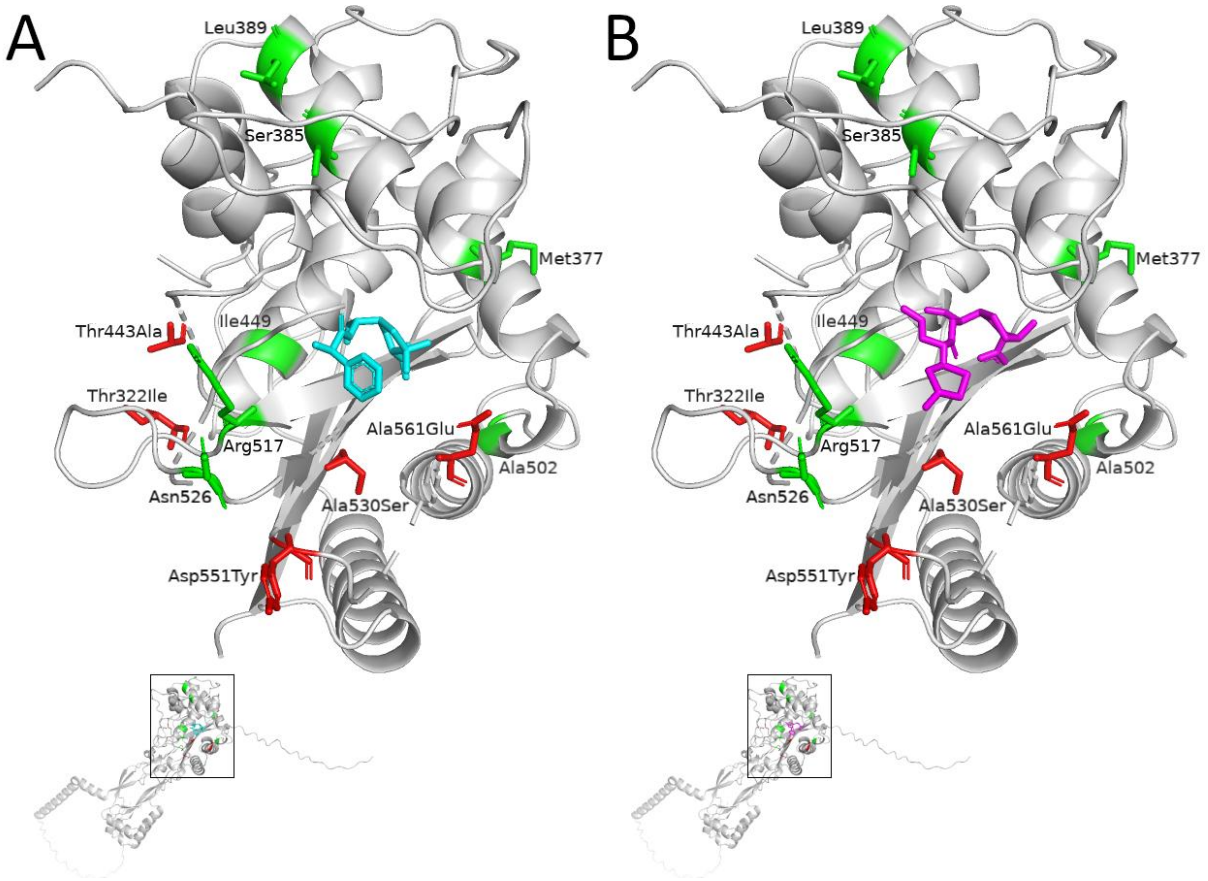

Figure 3: Crystal structure of transpeptidase domain (residues 254-610) of the penicillin binding protein 3 (PBP3) of *H. influenzae* (Bellini et al. [2019]) with superimposed ampicillin (A, colored in cyan) and cefotaxime (B, colored in magenta) molecules. *In vitro* selected amino acid substitutions in PBP3 Thr332Ile, Thr443Ala, Ala530Ser, Asp551Tyr, and Ala561Glu are colored in red. Known positions for amino acid substitutions defining established PBP3 resistance groups are colored in green.

307 Surprisingly, clones isolated from populations exposed to ceftriaxone (replicate 1 and replicate 3) did
308 not harbor any mutations in *ftsI.* However, we repeatedly selected different mutations in the *outer*
309 *membrane protein P2 (ompP2)*, i.e. p.Thr126fs (c.376_377insT), p.Val353fs (g.902541_902708del), as
310 well as a structural re-arrangement comprising a genomic inversion starting at codon 353 resulting in
311 p.Gly354fs (g.902541_902708inv). The latter two mutations were not detected with the short read
312 reference mapping approach but were identified based on the long read assemblies. However, both
313 mutations could also be detected in clones, for which no long read sequencing data were available,

314 through a manual check of the BWA alignments. In addition, various tandem repeat variations in
315 different genes could be detected using the long read sequencing data (Supplementary Table S2).
316 Mutation p.Thr126fs introduces a stop codon at position 129 in *ompP2*, resulting in a truncated protein
317 of only 128 amino acid instead of 359 amino acid (Supplementary Figure S4). The other two mutations
318 starting at codon 353 (i.e. g.902541_902708inv and g.902541_902708del) affect the C-terminus of
319 OmpP2, specifically the last β-strand of the β-barrel (Supplementary Figure S5). The mutation
320 g.902541_902708inv evolved independently in two replicate experiments. All three *ompP2* mutations
321 were significantly (p_{adj} < 4E-05) associated with a MIC increase against all three beta-lactam antibiotics
322 with a more pronounced effect for ceftriaxone susceptibility (i.e. 11.5-fold MIC increase, as compared
323 to 2-fold and 3.9-fold increase for ampicillin and cefotaxime, respectively). Still, all MIC increases
324 associated with *ompP2* mutations were below the respective EUCAST clinical breakpoints
325 (Supplementary Table S4). Interestingly, heteroresistance was observed for strains harboring the
326 inversion mutation (g.902541_902708inv) resulting in p.Gly354fs. Respective strains showed two
327 ellipses for all three beta-lactams on the agar plates with gradient diffusion strips (Supplementary
328 Figure S6). The lower MIC corresponded to the MIC observed for the parental strain ± two doubling
329 dilutions.

330 Besides mutations in *ftsI* and *ompP2*, we detected 13 different mutations in *pnp* (encoding
331 polyribonucleotide nucleotidyltransferase) in clones with and without pre-existing *ftsI* or *ompP2*
332 mutations isolated from populations exposed to cefotaxime, and in two replicated experiments under
333 ceftriaxone. Of those 13 mutations, seven induced a premature stop codon (p.Glu18*, p.Lys47*,
334 p.Glu80*, p.Gln159*, p.Glu220*, p.Glu471*, p.Met601*), three resulted in a frameshift (p.Val423fs,
335 p.Gly444fs, p.Glu580fs) and three were non-synonymous SNPs (p.Ala440Val, p.Gln505Lys,
336 p.Gly626Cys). p.Glu220* and p.Glu580fs were associated with a significant (p_{adj} < 0.034) MIC increase
337 for all three beta-lactams in clones with p.Thr126fs in OmpP2 (Supplementary Table S4). The effect of
338 the other detected mutations in *pnp* could not be determined due to an insufficient number of clones
339 carrying the specific mutation pattern. Four different mutations in *rpoB* (encoding DNA-directed RNA
340 polymerase subunit beta), three of them in close proximity (p.Leu149Phe, p.Arg151His, p.Gly154Asp),
341 were detected in clones isolated from populations exposed to ampicillin and ceftriaxone (replicate 2).
342 Furthermore, clones derived from ampicillin, cefotaxime, and ceftriaxone (replicate 2) exposed
343 populations evolved four different mutations in *udk* (encoding uridine kinase) and *spoT* (encoding
344 Guanosine-3',5'-bis(diphosphate) 3'-pyrophosphohydrolase). Two mutations in *prs* (encoding ribose-
345 phosphate pyrophosphokinase) were detected in ampicillin exposed clones as well as two mutations
346 in Rd_08000 (encoding a putative TonB-dependent receptor) in ceftriaxone exposed clones (replicate

347 1 and 3). However, only minor effects were observed, with a maximum median MIC fold increase of 3
348 for mutations in genes other than *ftsI* and *ompP2*.

349 Evolved resistant mutants pay a fitness cost under drug-free conditions

350 To investigate possible fitness costs of specific mutants and identify putative compensatory mutations
351 that minimize the fitness costs imposed by resistance-associated mutations, a competitive growth
352 assay was performed. Most of the evolved clones exhibited a lower fitness compared to the parental
353 strain (Figure 4 and Supplementary Table S1), strongly indicating an evolutionary trade-off between
354 resistance and competitive fitness in the absence of antibiotics. However, three strains
355 (E_0.5Amp_07a, E_1Amp_17a and E_0.032Ctx_07a) did not show a fitness/growth defect. One of
356 these clones (E_0.5Amp_07a) harbored putative beta-lactam susceptibility decreasing mutations in

357 *ftsI* and *rpoB* (26–28) accompanied by a mutation in *udk*. Another clone (E_1Amp_17a) showed the

358 same mutation pattern but with additional mutations in *rpoA*, *plsB*, and *prs*.

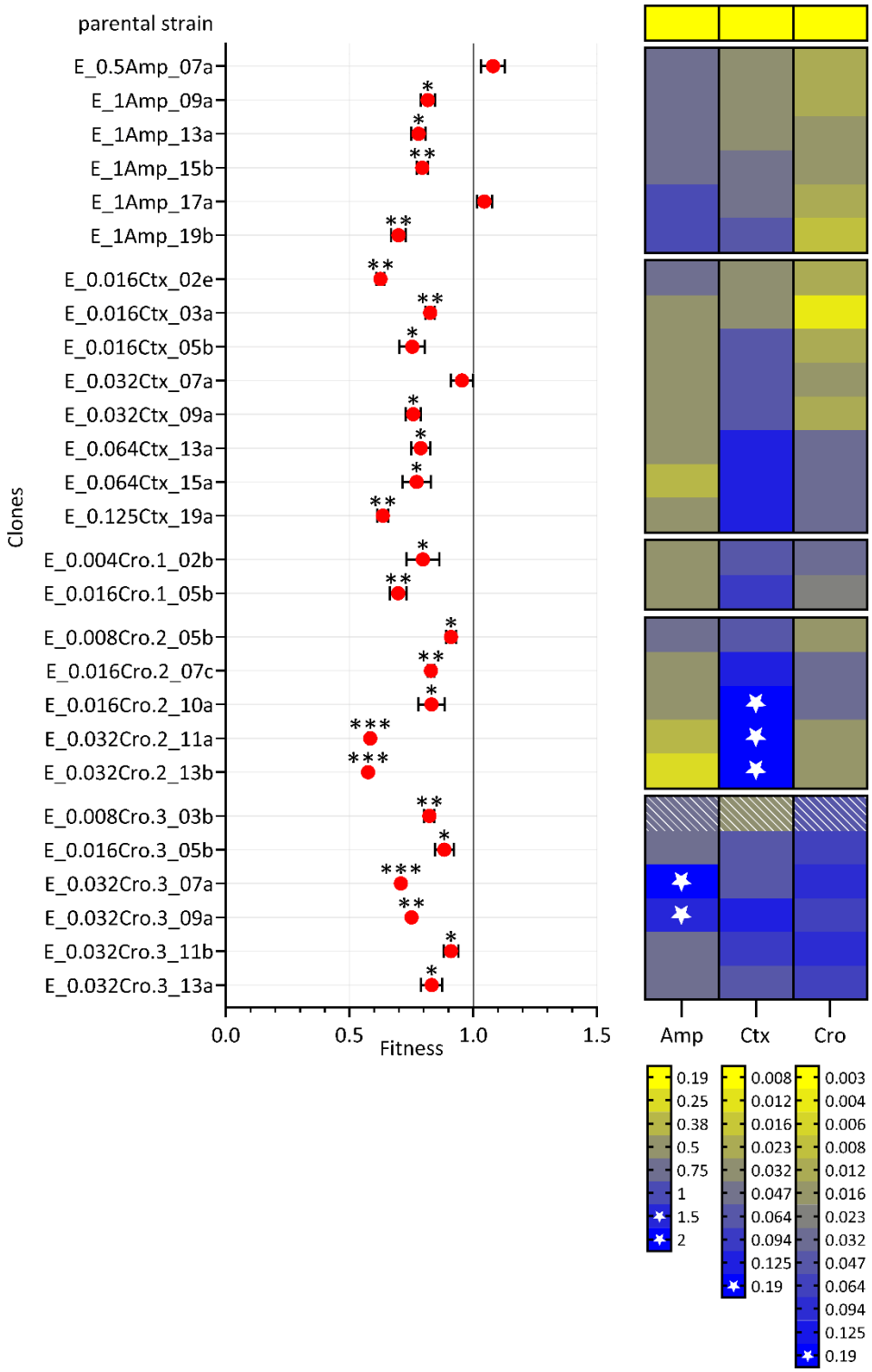

Figure 4: Bacterial fitness of selected clones derived from evolving populations exposed to ampicillin, cefotaxime, and ceftriaxone. Bacterial fitness measured as relative growth difference between the ancestral strain (*H. influenzae* Rd KW20) and the selected clone. A relative fitness of 1 indicates no fitness cost, whereas a value greater or less than 1 indicates increased or decreased fitness, respectively. The black bars represent standard deviation. *p_{adj}<0.05; **p_{adj}<0.01; ***p_{adj}<0.001. The heatmap indicates MIC values of ampicillin (Amp), cefotaxime (Ctx) and ceftriaxone (Cro) in mg/L of the respective strain (already presented in Figure 2). Stars indicate clinical resistance above the respective EUCAST breakpoints. Hatched panels indicate heteroresistance. Clones that derived from the same evolution experiment are grouped together on the y-axis.

359 Pairwise t-tests were conducted to compare all clones from a given evolution experiment. Particularly
360 interesting are comparisons between clones that differ by only a single mutation, as these allow for
361 the evaluation of fitness effects of individual mutations within a specific genetic background.
362 Comparison of fitness assay results of E_1Amp_17a and E_1Amp_13a revealed, that the *rpoA* mutation
363 restored wild-type fitness level in the respective mutational background (Supplementary Table S5).
364 Clone E_0.032Ctx_07a exhibits putative beta-lactam susceptibility decreasing mutations in *ftsI* and *pnp*
365 (29,30) accompanied by mutated *plsB*. In this case, comparison with fitness assay results of
366 E_0.016Ctx_05b, revealed that evolution of the *plsB* mutation resulted in wild-type fitness in the
367 respective mutational background. Moreover, fitness decrease could directly be addressed to and
368 quantified for specific mutations in *ftsI* (p.Asp551Tyr), *ompP2* (p.Thr126fs, p.Val353fs), and *pnp*
369 (p.Glu580fs, p.Glu220*). Correlating MIC increases and relative fitness of evolved clones revealed a
370 negative correlation between MIC and fitness for cefotaxime (coefficient = -0.45, p = 0.019), but no
371 correlation of MICs and fitness for ampicillin and ceftriaxone (Supplementary Table S6).

372 Evolved beta-lactam resistance is commonly associated with collateral sensitivity towards 373 aminoglycosides, clarithromycin, vancomycin, and colistin

374 To assess the expression of collateral effects, we characterized resistance to 14 antibiotics from
375 different classes for 17 clones isolated from the evolution experiments. We identified a consistent
376 pattern of decreased susceptibility for beta-lactam antibiotics (Figure 5). This also includes increased
377 MICs of the carbapenem meropenem. In this case, two clones (E_1Amp_10b and E_1Amp_19b) with
378 increased MICs of ampicillin, cefotaxime and ceftriaxone expressed cross-resistance to meropenem at
379 above EUCAST breakpoint levels. Surprisingly, two clones evolved under ceftriaxone exposure
380 exhibited increased susceptibility (i.e., collateral sensitivity) to meropenem. These two clones
381 additionally showed collateral sensitivity towards all non-beta-lactam antibiotics, excluding
382 tetracycline. In general, collateral sensitivity is most often expressed towards the three considered
383 aminoglycoside drugs (amikacin, kanamycin, and gentamicin), towards the macrolide clarithromycin,
384 as well as the polymyxin drug colistin, possibly indicating a robust emergence of collateral sensitivity
385 upon beta-lactam resistance evolution in *H. influenzae*.

386 Moreover, the two identified heteroresistant OmpP2 mutants consistently expressed heteroresistance
387 (i.e. two ellipses with a gradient diffusion test) towards a variety of antibiotics, including next to the
388 beta-lactams also fluoroquinolones, rifampicin and tetracycline.

389

390

391

392

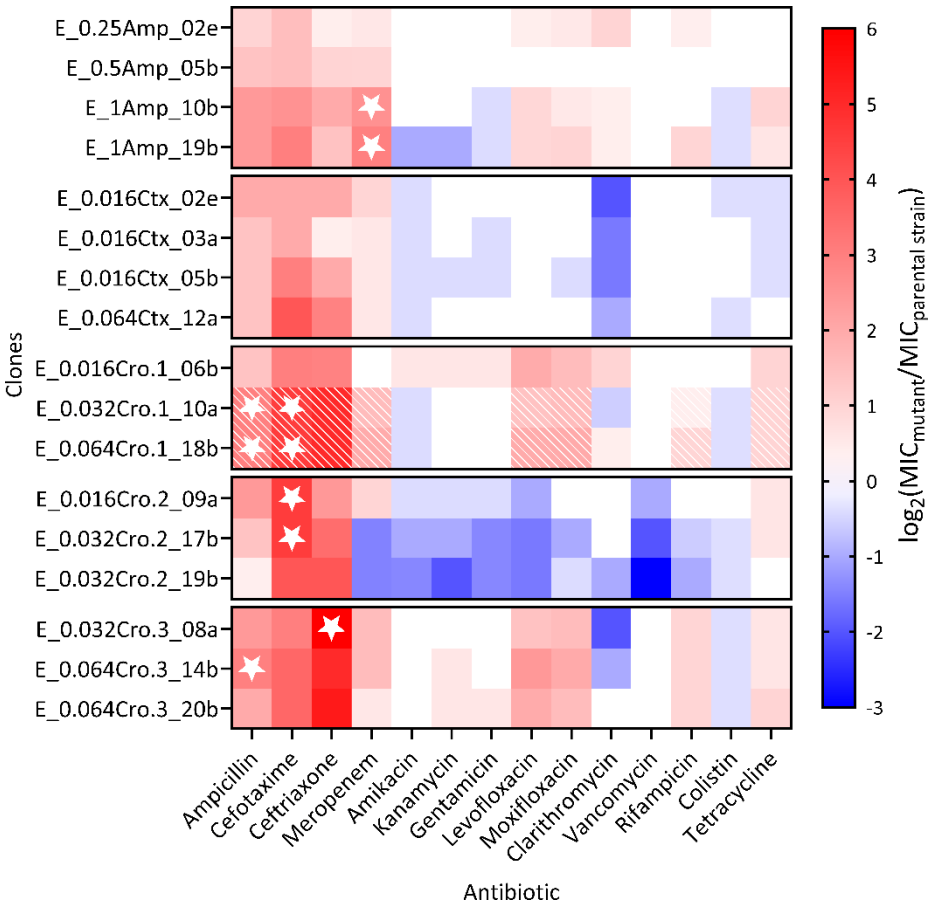

Figure 5: Collateral effects of increased MICs against individual beta-lactam antibiotics. Heat map of log_2-transformed relative increase in MIC of ampicillin, cefotaxime, ceftriaxone (underlying MIC values already presented in Figure 1), meropenem (beta-lactams), amikacin, kanamycin, gentamicin (aminoglycosides), levofloxacin, moxifloxacin (fluoroquinolones), clarithromycin (macrolide), vancomycin (glycopeptide), rifampicin (ansamycin), colistin (polymyxin) and tetracycline (tetracycline) in mutant clones relative to the MIC of the parental strain *H. influenzae* Rd KW20. Selected clones were evolved in the multi-step evolution experiment. Stars indicate clinical resistance above the respective EUCAST breakpoints (not available for aminoglycosides, clarithromycin, vancomycin, and colistin). Hatched panels indicate heteroresistance. Clones that derived from the same evolution experiment are grouped together on the y-axis.

393 ## Discussion

394 This study characterizes the *in vitro* evolution of resistance against three clinically relevant beta-lactam
395 antimicrobials in the opportunistic human pathogen *H. influenzae*. Our results revealed a linear
396 increase in the number of mutations across time that translated into rapid increases in resistance
397 against the treatment antibiotic. These increases in resistance are mainly mediated by mutations in
398 previously characterized AMR genes and, in two populations, is additionally associated with the
399 emergence of phenotypic heterogeneity in the form of antimicrobial heteroresistance. Importantly,
400 evolved resistance against one antibiotic caused significant fitness reductions in drug-free
401 environments and led to altered phenotypic responses to other drug classes, including numerous cases
402 of collateral sensitivity, especially towards aminoglycosides and additional drug classes. Understanding
403 evolutionary pathways and predicting their impact on future treatment regimens will be crucial to
404 reduce bacterial adaptation and selection of antimicrobial resistances.

405 Respiratory infections with *H. influenzae* are usually treated with an aminopenicillin in combination
406 with a beta-lactamase inhibitor (to overcome beta-lactamase mediated resistance). In case of
407 treatment failure or for severe invasive infections such as sepsis or meningitis, the use of third
408 generation cephalosporins such as cefotaxime and ceftriaxone is endorsed. However, it is only poorly
409 investigated to which extent for instance ampicillin resistance-causing genomic mutations affect
410 susceptibilities to third-generation cephalosporins and other last resort drugs. Furthermore, while
411 resistance to ceftriaxone and cefotaxime is currently rare in clinical isolates (31), understanding
412 potential evolutionary pathways to resistance and collateral effects is crucial for anticipating future
413 threats and optimizing treatment strategies.

414 To address this, we performed *in vitro* evolution experiments by exposing *H. influenzae* Rd KW20 to
415 increasing concentrations of ampicillin, cefotaxime, and ceftriaxone and monitored genomic changes.
416 Except for p.Thr322Ile, all PBP3 substitutions that were identified in these experiments, were
417 previously reported (in combination with other amino acid substitutions) for patient-derived isolates,
418 and exhibiting decreased susceptibility to cephalosporins and/or ampicillin (p.Thr443Ala (32–35),
419 p.Ala530Ser (32,33,35–38), p.Asp551Tyr (32) and p.Ala561Glu (37)). Notably, none of the PBP3
420 resistance group-defining mutations (p.Met377Ile, p.Ser385Thr, p.Leu389Phe, p.Ile449Val,
421 p.Ala502Val/Thr, p.Arg517His and p.Asn526Lys) evolved in the evolution experiments, although
422 p.Arg517His and p.Asn526Lys are two well-known driver mutations for ampicillin and cefotaxime
423 resistance (39,40). However, PBP3 p.Thr322Ile and p.Thr443Ala, that evolved under cefotaxime
424 exposure, are in close spatial proximity of Asn526 and Arg517, respectively. Interestingly, the resulting
425 structural changes in the beta-lactam binding site of PBP3, seem to mainly affect resistance to
426 cephalosporins rather than ampicillin. In *in vitro* evolution experiments with NTHi performed by Jakubu

427 et al.(41), one strain with wild-type *ftsI* evolved p.Thr443Ala in the presence of the cephalosporine
428 cefuroxime. In accordance with our results, the respective population showed only a MIC increase for
429 the cephalosporine, but not ampicillin. Hence, cephalosporins can select for amino acid substitutions
430 that do not affect ampicillin susceptibility.

431 However, we also observed convergent evolution of p.Ala530Ser under both ampicillin and cefotaxime
432 selection pressure. Respective clones showed significantly increased MICs especially of ampicillin and
433 ceftriaxone demonstrating that amino acid substitution in PBP3 can show collateral effects for
434 beta-lactam antibiotics. This indicates that the use of third generation cephalosporins for the
435 treatment of infections with ampicillin resistant isolates might be unsuccessful in some cases. Further
436 studies, that elucidate to what extent specific *ftsI* mutations and mutation patterns affect third
437 generation cephalosporin susceptibility as well as information on treatment outcome are essential to
438 evaluate this and improve clinical decision making.

439 Interestingly, we also observed clones with highly increased beta-lactam MICs that did not harbor any
440 *ftsI* mutations. Ceftriaxone exposure led to evolution of three different *ompP2* mutations resulting in
441 a profound effect on MICs of all three beta-lactam antibiotics. OmpP2 is one of the major outer
442 membrane proteins in *H. influenzae* with a mass of approximately 36 to 42 kDa. The protein functions
443 as a porin with an exclusion limit of about 1.4 kDa (42,43). Studies analyzing the *ompP2* gene of *H.*
444 *influenzae* reported a high conservation of the 16 β-strands building up the β-barrel, but increased
445 variation and accumulation of SNPs in the eight surface-exposed loop regions (44–47), which can result
446 in antigenic variation (48,49). By expression of OmpP2 and the AcrAB (multidrug efflux pump) encoding
447 genes of *H. influenzae* in an *acrB* and *ompF* knockout strain of *Escherichia coli*, Zwarma et al. provided
448 evidence that sensitivity to beta-lactams in *H. influenzae* actually is affected by OmpP2. While the
449 efflux pump AcrAB-TolC actively transports antibiotics from the cytoplasm and periplasm out of the
450 cell, OmpP2 counterbalances this efflux by leaking the drugs back into the cell (50).

451 Our findings confirm that diverse mutations in *ompP2* can significantly contribute to highly increased
452 beta-lactam MICs in *H. influenzae* (47,51,52). These *ompP2* mutations seem to be particularly selected
453 under ceftriaxone exposure. The *ompP2* frameshift mutation p.Thr126fs detected in this study resulted
454 in a stop codon at amino acid position 129 (instead of position 361) and therefore probably generated
455 a non-functional protein. The other two mutations resulting in p.Val353fs (deletion) and p.Gly354fs
456 (inversion) affected only the last β-strand of the porin, though AlphaFold predicted the mutated
457 sequence to not alter the β-barrel structure. Therefore, decreased influx of beta-lactam antibiotics
458 might have resulted from an altered electrostatic profile within the porin channel due to residue
459 properties of the changed AAs (53–55). Most studies on beta-lactam resistance in *H. influenzae* focus

460 on PBP3, which makes evaluation of the clinical relevance of *ompP2* mutations and their contribution
461 to treatment failure difficult.

462 Additional genes, with possibly more moderate effects on ampicillin, cefotaxime, and/or ceftriaxone
463 susceptibility are *rpoB*, *pnp*, and *spoT*. Mutations in these three genes have already been associated
464 with antibiotic resistance in other studies (56) or were selected in comparable evolution experiments
465 with *H. influenzae* (41,52), *E. coli* (57), and *Staphylococcus aureus* (58). RNA polymerase subunit β is
466 essential for transcription and even though specific mutations in *rpoB* are known to cause rifampicin
467 resistance, the gene was also recently associated with beta-lactam susceptibility in *Neisseria*
468 *gonorrhoeae* (26), *S. aureus* (27), and *Bacillus subtilis* (28). The highly conserved PNPase, which
469 influences mRNA and small RNA stability, is described to affect resistance and tolerance to
470 ciprofloxacin and aminoglycosides in *Pseudomonas aeruginosa*, respectively (29,30). The
471 pyrophosphohydrolase encoded by *spoT* synthesizes and hydrolyzes alarmone ppGpp, which induces
472 the expression of stress resistance components, and is involved in resistance and tolerance against
473 different antibiotics including beta-lactams for example in *P. aeruginosa* and *Helicobacter pylori* (59–
474 61). In our study, the effect of mutations in *rpoB, pnp and spoT* genes was limited to a two-fold MIC
475 increase. Therefore, one of the detected mutations alone does not result in beta-lactam resistance.
476 However, these novel association with decreased beta-lactam susceptibility in *H. influenzae* highlight
477 the complex interplay of various genetic factors in resistance mechanisms.

478 Drug resistance mutations often entail a reduced fitness in the absence of antibiotic pressure (62,63)
479 as the antibiotic target is often involved in important cellular processes (64). Indeed, almost all of the
480 clones examined exhibited a significant fitness deficit, with significant variability across mutants.
481 Notably, mutations associated with a higher increase in MIC do not necessarily entail a greater fitness
482 deficit. This is exemplified by the amino acid substitution p.Asp551Tyr in PBP3, which resulted in only
483 a moderate fitness decrease of approximately 9% (within the wild-type genomic background) but was
484 associated with an 8-fold increase of the MIC of ceftriaxone. Fitness levels can influence the
485 evolutionary success of a mutant. It is assumed that mutants with little or no fitness deficit tend to be
486 more successful (65). This is supported by studies on *Mycobacterium tuberculosis* and *Staphylococcus*
487 *aureus*, which discovered mutations with the lowest fitness costs to be the ones most frequently
488 identified in resistant clinical isolates (66–68).

489 In addition, the frameshift mutation in *ompP2* was associated with a relatively moderate fitness deficit
490 of approximately 12%. At the same time, this mutation provided a significant advantage in the
491 presence of the antibiotic, with a 23.5-fold increase in the MIC of ceftriaxone. In the evolution
492 experiment, the *ompP2* frameshift mutations outcompeted the inversion mutant over time, as both
493 mutations were initially detected in the second passage, but just the frameshift mutation persisted

494 until passage 20. However, applied bottlenecks, such as the 1:100 dilution used for passaging in this
495 study, inherently impose a random selection, as only a small, randomly chosen subset of the growing
496 population can proliferate in the next passage, thus increasing the effect of genetic drift. Genetic drift
497 influences the manifestation of specific mutations, as certain variants may be lost or
498 disproportionately represented purely by chance (69–71). A specificity of OmpP2 for NAD as well as
499 highly reduced uptake of NAD in *ompP2* knockout strains has been described for *H. influenzae* (72).
500 This might explain the reduced fitness observed for clones with mutated *ompP2*, as *H. influenzae* is
501 dependent on extracellular NAD (73) due to the lack of enzymes necessary for de novo biosynthesis
502 (74).

503 In cases of entailed fitness costs, fitness can be restored by reverting the resistance causing mutation,
504 which is just possible in the absence of antibiotic pressure (75), and by the acquisition of compensatory
505 mutations (62). We identified that the p.Thr443Ala substitution in PBP3 mitigates the fitness deficit
506 caused by p.Ala530Ser in PBP3 (and p.Val423fs in *pnp*), while this amino acid substitution is also
507 associated with a slight increase in the MIC of third-generation cephalosporins. Such mutations likely
508 present an increased risk for being selected in the presence and the absence of the antibiotic.

509 Resistance-conferring mutations can additionally affect susceptibility to other antibiotics.
510 Simultaneously acquired resistance to another antibiotic is referred to as cross-resistance, while
511 collateral sensitivity describes an evolutionary trade-off where antibiotic resistance to one antibiotic
512 confers increased susceptibility to another antibiotic. Robust collateral sensitivity phenotypes could
513 help to develop new evolutionary-based treatment strategies and therefore may reduce resistance
514 emergence (76).

515 We observed collaterally increased MICs of fluoroquinolones in *ompP2* mutated clones with decreased
516 beta-lactam susceptibility. This influence of OmpP2 on fluoroquinolone susceptibility in *H. influenzae*
517 is supported by evolution experiments with clinical isolates of *H. influenzae* in the presence of
518 moxifloxacin that selected for *ompP2* mutations and MICs exceeding CLSI breakpoints for moxifloxacin
519 (52). In our experiments MICs did not exceed EUCAST clinical breakpoints for moxifloxacin (> 0.125
520 mg/L) and levofloxacin (> 0.06 mg/L). However, the success of treatment with fluoroquinolones might
521 be reduced in these cases. For the macrolide clarithromycin we observed differential effects in the
522 *ompP2* mutants.

523 Overall, our study identified the emergence of collateral sensitivity towards the three tested
524 aminoglycosides, against the macrolide clarithromycin, the glycopeptide vancomycin, and also the
525 polymyxin drug colistin. Especially the reduced MIC to vancomycin in one evolution experiment was
526 surprising as this antibiotic is only active against gram positive bacteria. This effect might be linked to
527 a mutated *mltC* gene, that has already been associated with increased susceptibility to vancomycin

528 under acidic pH in a MltC/MltE deletion mutant of *Escherichia coli* (77). Overall, these patterns of
529 evolved collateral sensitivity were observed for more than 50% of the tested clones. Even though they
530 did not emerge in all cases, collateral sensitivities seem to occur frequently towards specific antibiotics
531 and may thus be a promising focus for optimizing antibiotic treatment designs.

532 The therapeutic potential of such evolutionary trade-offs clearly deserves further study, especially
533 using combinatorial and sequential treatments with a beta-lactam and an aminoglycoside or
534 clarithromycin. Unfortunately, due to the ototoxicity and nephrotoxicity which are common side
535 effects of aminoglycosides, a potential combinatorial or alternating treatment would not be
536 appropriate for simple respiratory tract infections caused by *H. influenzae* (78), but rather of value for
537 severe infections like meningitis or sepsis. In fact, beta-lactam–aminoglycoside combinations are used
538 in cases like neonatal meningitis or severe sepsis of unknown etiology, where *H. influenzae* is only
539 rarely the causative pathogen. Nevertheless, in such cases, according to our findings this therapy could
540 be effective.

541 Conclusion

542 Overall, this study revealed the fast evolution of beta-lactam resistance in the opportunistic human
543 pathogen *H. influenzae*. Evolved resistance is mediated by an accumulation of mutations in known
544 target genes and in two populations associated with the emergence of heteroresistance. Almost all
545 resistant clones suffered from reduced competitive fitness in the absence of antibiotics and often
546 expressed collateral sensitivity towards other drug classes, especially aminoglycosides. These findings
547 indicate robust evolutionary trade-offs that are caused by the resistance-conferring mutations and
548 may represent a promising focus for optimizing antibiotic treatment designs. Similarly, a further
549 analysis of novel resistance mutations and of epistatic effects may additionally assist to improve the
550 development of new antimicrobial treatment strategies.

551 Acknowledgments

552 We thank T. Niemann, V. Mohr, M. Mundzeck, T. Struve from the Research Center Borstel, Germany
553 for excellent technical assistance.

554 Funding

555 We are grateful for financial support from the German Science Foundation within the Research and
556 Training Group 2501 (RTG 2501) on Translational Evolutionary Research (project 4.2, to HS; and
557 associated doctoral project of SP), the Max-Planck Society (Fellowship to HS), the Deutsche
558 Forschungsgemeinschaft (DFG, German Research Foundation) under Germanys Excellence Strategy –
559 EXC 2167 Precision Medicine in Inflammation, the German Ministry of Education and Research (BMBF)

560 for the German Center of Infection Research (DZIF), and the Leibniz Science Campus Evolutionary
561 Medicine of the LUNG (EvoLUNG).

562 Transparency Declaration

563 The authors declare that they do not have any competing interests.

564 Author contributions

565 SP, MD and MM conceived the study. SP performed evolutionary experiments, phenotyping and
566 statistical analysis. MM performed Bayesian clock dating analysis. SP, MD, and CU performed next
567 generation sequencing. SP and MM wrote the first draft, all authors reviewed the manuscript, and
568 provided intellectual input. All authors read and approved the final manuscript.

569 References

570 1. Antimicrobial Resistance Collaborators. Global burden of bacterial antimicrobial resistance in
571 2019: a systematic analysis. Lancet Lond Engl. 2022 Feb 12;399(10325):629–55.

572 2. WHO bacterial priority pathogens list, 2024: Bacterial pathogens of public health importance to
573 guide research, development and strategies to prevent and control antimicrobial resistance
574 [Internet]. [cited 2024 Oct 18]. Available from:
575 https://www.who.int/publications/i/item/9789240093461

576 3. Clark SE. Commensal bacteria in the upper respiratory tract regulate susceptibility to infection.
577 Curr Opin Immunol. 2020 Oct;66:42–9.

578 4. Teo SM, Mok D, Pham K, Kusel M, Serralha M, Troy N, et al. The Infant Nasopharyngeal
579 Microbiome Impacts Severity of Lower Respiratory Infection and Risk of Asthma Development.
580 Cell Host Microbe. 2015 May 13;17(5):704–15.

581 5. Tsang RSW, Ulanova M. The changing epidemiology of invasive *Haemophilus influenzae* disease:
582 Emergence and global presence of serotype a strains that may require a new vaccine for control.
583 Vaccine. 2017 Jul 24;35(33):4270–5.

584 6. Whittaker R, Economopoulou A, Dias JG, Bancroft E, Ramliden M, Celentano LP. Epidemiology of
585 invasive *Haemophilus influenzae* disease, Europe, 2007–2014. Emerg Infect Dis J. 2017;23(3):396.

586 7. Heinz E. The return of Pfeiffer's bacillus: Rising incidence of ampicillin resistance in *Haemophilus*
587 *influenzae*. Microb Genomics. 2018;4(9).

588 8. Zhou M, Fu P, Fang C, Shang S, Hua C, Jing C, et al. Antimicrobial resistance of *Haemophilus*
589 *influenzae* isolates from pediatric hospitals in Mainland China: Report from the ISPED program,
590 2017–2019. Indian J Med Microbiol. 2021 Oct 1;39(4):434–8.

591 9. Tsang RSW, Shuel M, Whyte K, Hoang L, Tyrrell G, Horsman G, et al. Antibiotic susceptibility and
592 molecular analysis of invasive Haemophilus influenzae in Canada, 2007 to 2014. J Antimicrob
593 Chemother. 2017 May 1;72(5):1314–9.

594 10. Red Book (2021): Report of the Committee on Infectious Diseases. American Academy of
595 Pediatrics; 2021.

596 11. Scriver SR, Walmsley SL, Kau CL, Hoban DJ, Brunton J, McGeer A, et al. Determination of
597 antimicrobial susceptibilities of Canadian isolates of *Haemophilus influenzae* and characterization
598 of their beta-lactamases. Antimicrob Agents Chemother. 1994;38(7):1678–80.

599 12. Farrell DJ, Morrissey I, Bakker S, Buckridge S, Felmingham D. Global distribution of TEM-1 and
600 ROB-1 β-lactamases in *Haemophilus influenzae*. J Antimicrob Chemother. 2005;56(4):773–6.

601 13. Parr TR, Bryan LE. Mechanism of resistance of an ampicillin-resistant, beta-lactamase-negative
602 clinical isolate of *Haemophilus influenzae* type b to beta-lactam antibiotics. Antimicrob Agents
603 Chemother. 1984;25(6):747–53.

604 14. Ubukata K, Shibasaki Y, Yamamoto K, Chiba N, Hasegawa K, Takeuchi Y, et al. Association of
605 amino acid substitutions in penicillin-binding protein 3 with β-lactam resistance in β-lactamase-
606 negative ampicillin-resistant *Haemophilus influenzae*. Antimicrob Agents Chemother.
607 2001;45(6):1693–9.

608 15. Jansen G, Barbosa C, Schulenburg H. Experimental evolution as an efficient tool to dissect
609 adaptive paths to antibiotic resistance. Drug Resist Updat Rev Comment Antimicrob Anticancer
610 Chemother. 2013 Dec;16(6):96–107.

611 16. Batra A, Roemhild R, Rousseau E, Franzenburg S, Niemann S, Schulenburg H. High potency of
612 sequential therapy with only β-lactam antibiotics. eLife. 2021 Jul 28;10:e68876.

613 17. Baym M, Kryazhimskiy S, Lieberman TD, Chung H, Desai MM, Kishony R. Inexpensive multiplexed
614 library preparation for megabase-sized genomes. PloS One. 2015;10(5):e0128036.

615 18. Kohl TA, Utpatel C, Schleusener V, De Filippo MR, Beckert P, Cirillo DM, et al. MTBseq: a
616 comprehensive pipeline for whole genome sequence analysis of Mycobacterium tuberculosis
617 complex isolates. PeerJ. 2018;6:e5895.

618 19. Li H, Durbin R. Fast and accurate short read alignment with Burrows-Wheeler transform.
619 Bioinforma Oxf Engl. 2009 Jul 15;25(14):1754–60.

620 20. McKenna A, Hanna M, Banks E, Sivachenko A, Cibulskis K, Kernytsky A, et al. The Genome
621 Analysis Toolkit: a MapReduce framework for analyzing next-generation DNA sequencing data.
622 Genome Res. 2010 Sep;20(9):1297–303.

623 21. Price MN, Dehal PS, Arkin AP. FastTree 2 – Approximately Maximum-Likelihood Trees for Large
624 Alignments. PLOS ONE. 2010 Mar 10;5(3):e9490.

625 22. Rambaut A, Lam TT, Max Carvalho L, Pybus OG. Exploring the temporal structure of
626 heterochronous sequences using TempEst (formerly Path-O-Gen). Virus Evol [Internet]. 2016 Jan
627 1 [cited 2017 Jun 14];2(1). Available from:
628 https://academic.oup.com/ve/article/2/1/vew007/1753488/Exploring-the-temporal-structure-
629 of-heterochronous

630 23. Bouckaert R, Vaughan TG, Barido-Sottani J, Duchêne S, Fourment M, Gavryushkina A, et al.
631 BEAST 2.5: An advanced software platform for Bayesian evolutionary analysis. PLOS Comput Biol.
632 2019 Apr 8;15(4):e1006650.

633 24. Wiser MJ, Lenski RE. A Comparison of methods to measure fitness in *Escherichia coli*. PLOS ONE.
634 2015 May 11;10(5):e0126210.

635 25. Abramson J, Adler J, Dunger J, Evans R, Green T, Pritzel A, et al. Accurate structure prediction of
636 biomolecular interactions with AlphaFold 3. Nature. 2024 Jun;630(8016):493–500.

637 26. Palace SG, Wang Y, Rubin DHF, Welsh MA, Mortimer TD, Cole K, et al. RNA polymerase
638 mutations cause cephalosporin resistance in clinical *Neisseria gonorrhoeae* isolates. Stallings CL,
639 Storz G, Shafer W, editors. eLife. 2020 Feb 3;9:e51407.

640 27. Panchal VV, Griffiths C, Mosaei H, Bilyk B, Sutton JAF, Carnell OT, et al. Evolving MRSA: High-level
641 β-lactam resistance in *Staphylococcus aureus* is associated with RNA Polymerase alterations and
642 fine tuning of gene expression. PLOS Pathog. 2020;16(7):e1008672.

643 28. Patel Y, Soni V, Rhee KY, Helmann JD. Mutations in *rpoB* that confer rifampicin resistance can
644 alter levels of peptidoglycan precursors and affect β-lactam susceptibility. mBio.
645 2023;14(2):e03168-22.

646 29. Fan Z, Chen H, Li M, Pan X, Fu W, Ren H, et al. *Pseudomonas aeruginosa* polynucleotide
647 phosphorylase contributes to ciprofloxacin resistance by regulating PrtR. Front Microbiol.
648 2019;10:1762.

649 30. Fan Z, Pan X, Wang D, Chen R, Fu T, Yang B, et al. *Pseudomonas aeruginosa* polynucleotide
650 phosphorylase controls tolerance to aminoglycoside antibiotics by regulating the MexXY
651 multidrug efflux pump. Antimicrob Agents Chemother. 2021 Jan 20;65(2).

652 31. Abavisani M, Keikha M, Karbalaei M. First global report about the prevalence of multi-drug
653 resistant Haemophilus influenzae: a systematic review and meta-analysis. BMC Infect Dis. 2024
654 Jan 15;24(1):90.

655 32. Osaki Y, Sanbongi Y, Ishikawa M, Kataoka H, Suzuki T, Maeda K, et al. Genetic approach to study
656 the relationship between penicillin-binding protein 3 mutations and *Haemophilus influenzae*
657 beta-lactam resistance by using site-directed mutagenesis and gene recombinants. Antimicrob
658 Agents Chemother. 2005 Jul;49(7):2834–9.

659 33. García-Cobos S, Campos J, Lázaro E, Román F, Cercenado E, García-Rey C, et al. Ampicillin-
660 resistant non-β-lactamase-producing *Haemophilus influenzae* in Spain: Recent emergence of
661 clonal isolates with increased resistance to cefotaxime and cefixime. Antimicrob Agents
662 Chemother. 2007;51(7):2564–73.

663 34. Straker K, Wootton M, Simm AM, Bennett PM, MacGowan AP, Walsh TR. Cefuroxime resistance
664 in non-β-lactamase *Haemophilus influenzae* is linked to mutations in *ftsI*. J Antimicrob
665 Chemother. 2003;51(3):523–30.

666 35. Slotved HC, Johannesen TB, Stegger M, Dalby T, Fuursted K. National Danish surveillance of
667 invasive clinical *Haemophilus influenzae* isolates and their resistance profile. Front Microbiol.
668 2023 Nov;14.

669 36. Skaare D, Allum AG, Anthonisen IL, Jenkins A, Lia A, Strand L, et al. Mutant *ftsI* genes in the
670 emergence of penicillin-binding proteinmediated β-lactam resistance in *Haemophilus influenzae*
671 in Norway. Clin Microbiol Infect. 2010 Aug 1;16(8):1117–24.

672 37. Thegerström J, Matuschek E, Su YC, Riesbeck K, Resman F. A novel PBP3 substitution in
673 *Haemophilus influenzae* confers reduced aminopenicillin susceptibility. BMC Microbiol. 2018
674 May 31;18(1):48.

675 38. Lâm TT, Claus H, Elias J, Frosch M, Vogel U. Ampicillin resistance of invasive *Haemophilus*
676 *influenzae* isolates in Germany 2009–2012. Int J Med Microbiol. 2015 Oct 1;305(7):748–55.

677 39. Diricks M, Petersen S, Bartels L, Lâm TT, Claus H, Bajanca-Lavado MP, et al. Revisiting mutational
678 resistance to ampicillin and cefotaxime in Haemophilus influenzae. Genome Med. 2024 Dec
679 4;16(1):140.

680 40. Skaare D, Anthonisen IL, Kahlmeter G, Matuschek E, Natås OB, Steinbakk M, et al. Emergence of
681 clonally related multidrug resistant Haemophilus influenzae with penicillin-binding protein 3-
682 mediated resistance to extended-spectrum cephalosporins, Norway, 2006 to 2013. Euro Surveill
683 Bull Eur Sur Mal Transm Eur Commun Dis Bull. 2014 Dec 11;19(49):20986.

684 41. Jakubu V, Vrbova I, Bitar I, Cechova M, Malisova L, Zemlickova H. Evolution of mutations in the
685 *ftsI* gene leading to amino acid substitutions in PBP3 in *Haemophilus influenzae* strains under the
686 selective pressure of ampicillin and cefuroxime. Int J Med Microbiol. 2024 Sep 1;316:151626.

687 42. Vachon V, D J Lyew, Coulton JW. Transmembrane permeability channels across the outer
688 membrane of *Haemophilus influenzae* type b. J Bacteriol. 1985;162(3):918–24.

689 43. Vachon V, Laprade R, Coulton JW. Properties of the porin of *Haemophilus influenzae* type b in
690 planar lipid bilayer membranes. Biochim Biophys Acta BBA - Biomembr. 1986 Jan 1;861:74–82.

691 44. Sikkema DJ, Murphy TF. Molecular analysis of the P2 porin protein of nontypeable *Haemophilus*
692 *influenzae*. Infect Immun. 1992;60(12):5204–11.

693 45. Duim B, Dankert J, Jansen HM, van Alphen L. Genetic analysis of the diversity in outer membrane
694 protein P2 of non-encapsulated *Haemophilus influenzae*. Microb Pathog. 1993 Jun 1;14(6):451–
695 62.

696 46. Bell J, Grass S, Jeanteur D, Munson RS. Diversity of the P2 protein among nontypeable
697 *Haemophilus influenzae* isolates. Infect Immun. 1994;62(6):2639–43.

698 47. Annette G. Regelink, David Dahan, Lieke V. M. Möller, James W. Coulton, Paul Eijk, Peter Van
699 Ulsen, et al. Variation in the composition and pore function of major outer membrane pore

700 protein P2 of *Haemophilus influenzae* from cystic fibrosis patients. Antimicrob Agents
701 Chemother. 1999;43(2):226–32.

702 48. Duim B, van Alphen L, Eijk P, Jansen HM, Dankert J. Antigenic drift of non-encapsulated
703 *Haemophilus influenzae* major outer membrane protein P2 in patients with chronic bronchitis is
704 caused by point mutations. Mol Microbiol. 1994 Mar 1;11(6):1181–9.

705 49. Duim B, Vogel L, Puijk W, Jansen HM, Meloen RH, Dankert J, et al. Fine mapping of outer
706 membrane protein P2 antigenic sites which vary during persistent infection by *Haemophilus*
707 *influenzae*. Infect Immun. 1996;64(11):4673–9.

708 50. Zwama M, Yamaguchi A, Nishino K. Phylogenetic and functional characterisation of the
709 *Haemophilus influenzae* multidrug efflux pump AcrB. Commun Biol. 2019 Sep 13;2(1):340.

710 51. Cherkaoui A, Diene SM, Renzoni A, Emonet S, Renzi G, François P, et al. Imipenem
711 heteroresistance in nontypeable *Haemophilus influenzae* is linked to a combination of altered
712 PBP3, slow drug influx and direct efflux regulation. Clin Microbiol Infect. 2017;23(2):118.e9-
713 118.e19.

714 52. Honda H, Sato T, Shinagawa M, Fukushima Y, Nakajima C, Suzuki Y, et al. *In vitro* derivation of
715 fluoroquinolone-resistant mutants from multiple lineages of *Haemophilus influenzae* and
716 identification of mutations associated with fluoroquinolone resistance. Antimicrob Agents
717 Chemother. 2020;64(2):10.1128/aac.01500-19.

718 53. Lou H, Chen M, Black SS, Bushell SR, Ceccarelli M, Mach T, et al. Altered antibiotic transport in
719 OmpC mutants isolated from a series of clinical strains of multi-drug resistant *E. coli*. PLoS One.
720 2011;6(10):e25825.

721 54. Raj Singh P, Ceccarelli M, Lovelle M, Winterhalter M, Mahendran KR. Antibiotic permeation
722 across the OmpF channel: Modulation of the affinity site in the presence of magnesium. J Phys
723 Chem B. 2012 Apr 19;116(15):4433–8.

724 55. Acosta-Gutierrez S, Scorciapino MA, Bodrenko I, Ceccarelli M. Filtering with electric field: The
725 case of *E. coli* porins. J Phys Chem Lett. 2015 May 21;6(10):1807–12.

726 56. Boonsiri T, Watanabe S, Tan XE, Thitiananpakorn K, Narimatsu R, Sasaki K, et al. Identification
727 and characterization of mutations responsible for the β-lactam resistance in oxacillin-susceptible
728 mecA-positive *Staphylococcus aureus*. Sci Rep. 2020 Oct 9;10(1):16907.

729 57. Card KJ, Thomas MD, Graves JL, Barrick JE, Lenski RE. Genomic evolution of antibiotic resistance
730 is contingent on genetic background following a long-term experiment with *Escherichia coli*. Proc
731 Natl Acad Sci. 2021 Feb 2;118(5):e2016886118.

732 58. Sulaiman Jordy E, Lam H. Novel daptomycin tolerance and resistance mutations in methicillin-
733 resistant *Staphylococcus aureus* from adaptive laboratory evolution. mSphere.
734 2021;6(5):10.1128/msphere.00692-21.

735 59. Wu J, Long Q, Xie J. (p)ppGpp and drug resistance. J Cell Physiol. 2010 Aug;224(2):300–4.

736 60. Nguyen D, Joshi-Datar A, Lepine F, Bauerle E, Olakanmi O, Beer K, et al. Active starvation
737 responses mediate antibiotic tolerance in biofilms and nutrient-limited bacteria. Science. 2011
738 Nov 18;334(6058):982–6.

739 61. Geng X, Li W, Chen Z, Gao S, Hong W, Ge X, et al. The bifunctional enzyme SpoT is involved in the
740 clarithromycin tolerance of *Helicobacter pylori* by upregulating the transporters HP0939,
741 HP1017, HP0497, and HP0471. Antimicrob Agents Chemother. 2017 May;61(5).

742 62. Andersson DI, Hughes D. Antibiotic resistance and its cost: is it possible to reverse resistance?
743 Nat Rev Microbiol. 2010 Apr 1;8(4):260–71.

744 63. Andersson DI, Levin BR. The biological cost of antibiotic resistance. Curr Opin Microbiol. 1999 Oct
745 1;2(5):489–93.

746 64. Melnyk AH, Wong A, Kassen R. The fitness costs of antibiotic resistance mutations. Evol Appl.
747 2015 Mar;8(3):273–83.

748 65. Hughes D, Andersson DI. Evolutionary trajectories to antibiotic resistance. Annu Rev Microbiol.
749 2017 Sep 8;71:579–96.

750 66. O'Neill AJ, Huovinen T, Fishwick CWG, Chopra I. Molecular genetic and structural modeling
751 studies of *Staphylococcus aureus* RNA polymerase and the fitness of rifampin resistance
752 genotypes in relation to clinical prevalence. Antimicrob Agents Chemother. 2006;50(1):298–309.

753 67. Böttger EC, Springer B, Pletschette M, Sander P. Fitness of antibiotic-resistant microorganisms
754 and compensatory mutations. Nat Med. 1998 Dec 1;4(12):1343–4.

755 68. Sander P, Springer B, Prammananan T, Sturmfels A, Kappler M, Pletschette M, et al. Fitness cost
756 of chromosomal drug resistance-conferring mutations. Antimicrob Agents Chemother.
757 2002;46(5):1204–11.

758 69. Gamblin J, Gandon S, Blanquart F, Lambert A. Bottlenecks can constrain and channel
759 evolutionary paths. Genetics. 2023;224(2):iyad001.

760 70. Wahl LM, Gerrish PJ. The probability that beneficial mutations are lost in populations with
761 periodic bottlenecks. Evolution. 2001;55(12):2606–10.

762 71. Mahrt N, Tietze A, Künzel S, Franzenburg S, Barbosa C, Jansen G, et al. Bottleneck size and
763 selection level reproducibly impact evolution of antibiotic resistance. Nat Ecol Evol. 2021
764 Sep;5(9):1233–42.

765 72. Andersen C, Maier E, Kemmer G, Blass J, Hilpert AK, Benz R, et al. Porin OmpP2 of *Haemophilus*
766 *influenzae* shows specificity for nicotinamide-derived nucleotide substrates. J Biol Chem. 2003 Jul
767 4;278(27):24269–76.

768 73. Evans NM, Smith DD, Wicken AJ. Haemin and nicotinamide adenine dinucleotide requirements
769 of *Haemophilus influenzae* and *Haemophilus parainfluenzae*. J Med Microbiol. 1974;7(3):359–65.

770 74. Fleischmann RD, Adams MD, White O, Clayton RA, Kirkness EF, Kerlavage AR, et al. Whole-
771 genome random sequencing and assembly of *Haemophilus influenzae* Rd. Science. 1995 Jul
772 28;269(5223):496–512.

773 75. Pennings PS, Ogbunugafor CB, Hershberg R. Reversion is most likely under high mutation supply
774 when compensatory mutations do not fully restore fitness costs. G3 GenesGenomesGenetics.
775 2022;12(9):jkac190.

776 76. Roemhild R, Andersson DI. Mechanisms and therapeutic potential of collateral sensitivity to
777 antibiotics. PLOS Pathog. 2021 Jan 14;17(1):e1009172.

778 77. Son JE, Park SH, Choi U, Lee CR. Lytic transglycosylase repertoire diversity enables intrinsic
779 antibiotic resistance and daughter cell separation in Escherichia coli under acidic stress.
780 Antimicrob Agents Chemother. 2024 Jun 17;68(7):e00372-24.

781 78. Le TA, Hiba T, Chaudhari D, Preston AN, Palowsky ZR, Ahmadzadeh S, et al. Aminoglycoside-
782 Related Nephrotoxicity and Ototoxicity in Clinical Practice: A Review of Pathophysiological
783 Mechanism and Treatment Options. Adv Ther. 2023 Apr 1;40(4):1357–65.

784

785

786 ## Supplementary Figures

787 Supplementary Figure S1: Graphical protocol of the performed multi-step evolution experiment
788 (generated with BioRender).

789 Supplementary Figure S2: Graphical protocol of the performed competitive growth assay (generated
790 with BioRender).

791 Supplementary Figure S3: Maximum likelihood phylogeny of *H. influenzae* Rd KW20 clones evolved in
792 the absence of an antibiotic pressure (A, 40 clones) and in three replicate populations evolved in
793 cefotaxime (B, replicate 1 with 57 clones; C replicate 2 with 56 clones; D, replicate 3 with 59 clones).
794 Amino acid substitutions in the penicillin binding protein 3 (PBP3) and presence of mutations in
795 specified genes as well as minimum inhibitory concentration (MIC) changes over time are color coded.
796 Strains that exceeded the clinical breakpoint for ampicillin/cefotaxime/ceftriaxone according to
797 EUCAST breakpoints are marked with a white star at the MIC heatmap.
798 The specified genes are those in which at least 20 clones from the whole set of selected clones
799 exhibited mutations but did not mutate under antibiotic-free conditions.

800 Supplementary Figure S4: Crystal structure of Outer membrane protein P2 of wild-type *H. influenzae*
801 Rd KW20 (A) and mutated OmpP2 (B) truncated due to p.Thr126fs (c.376_377insT). Structures were
802 predicted using the AlphaFold Server powerd by AlphaFold 3 (26) and visualized using PyMOL v3.0.
803 Deviations between the two variants are highlighted in red.

804 Supplementary Figure S5: Crystal structure of Outer membrane protein P2 of wild-type *H. influenzae*
805 Rd KW20, shown in side view (A) and bottom view (B) and two variants of OmpP2 altered due to
806 p.Gly354fs (C and D, inversion) and p.Val353fs (E and F, deletion). Structures were predicted using the
807 AlphaFold Server powerd by AlphaFold 3 (26) and visualized using PyMOL v3.0. Deviations between
808 the two variants are labeled and highlighted in yellow (hydrophobic), green (polar uncharged), and
809 blue (positively charged).

810 Supplementary Figure S6: Gradient diffusion test demonstrating heteroresistance. The image shows
811 two distinct inhibition zones surrounding the antibiotic gradient strip, indicative of a heteroresistant
812 bacterial population. The inner zone corresponds to a subpopulation with higher antibiotic resistance,
813 while the outer zone represents the more susceptible majority.